High resolution (20 cycles/mm) digital X-ray mammography using amorphous Selenium directly coupled to CCD readout devices

David M. Hunter[a], Gueorgui Belev[b], Giovanni DeCrescenzo[a], Safa O. Kasap[b], James G. Mainprize[a], Gordon Mawdsley[a], John A. Rowlands[a], Charles Smith[c], Vladimir Verpakhovski[a], Shi Yin[d], and Martin J. Yaffe[a]

[a]Department of Medical Biophysics, University of Toronto, Sunnybrook & Women's College Health Sciences Centre, 2075 Bayview Avenue, Toronto, Ontario, M4N 3M5, Canada

[b]Department of Electrical Engineering, University of Saskatchewan,57 Campus Dr., Saskatoon, Saskatchewan, S7N 5A9, Canada

[c]DALSA Inc., 605 McMurray Road, Waterloo, Ontario, N2V 2E9, Canada

[d]Nova R&D, Riverside, California, 92507-3429, USA

ABSTRACT

We describe a simple, single row, X-ray detector that utilizes 200 μm thick layers of amorphous Selenium (a-Se) directly deposited on a specially-designed CCD (charge coupled device) with a 25 μm del (detector element) pitch. The simple detector, which in itself is not directly applicable to mammography, has been used to test the feasibiltity of creating digital mammography detectors by directly depositing a-Se onto a CCD readout device. To enable the use of electron transport CCDs with a-Se layers we have developed special a-Se hole blocking layers which permit the transfer of electrons to the CCD while suppressing the development of hole leakage current in the presence of the high negative bias ($\sim$1000 V) required to make the a-Se X-ray sensitive. We report measurements of the charge transfer efficiency (CTE), dark signal, X-ray sensitivity, X-ray signal linearity, and X-ray MTF (modulation transfer function) of the simple detector. As the thickness of the a-Se hole blocking layer is increased, the MTF decreases. For a thin ($\leq 1\mu$m) blocking layer the MTF at a spatial frequency of 20 mm^{-1} was about 0.4, which introduces noise aliasing. In the design of a slot scan selenium CCD TDI detector, the blocking layer thickness will be chosen to suppress noise aliasing in a manner which shall optimize the DQE (detective quantum efficiency).

Keywords: digital mammography, X-ray detectors, high resolution, selenium, CCD

1. INTRODUCTION

Digital mammography may be achieved using full field or slot-scanned imaging systems. These different approaches have been described elsewhere.[1–4] The number of detector elements (dels) required in full field designs for a standard 18 cm x 24 cm field are: 4.3 x 10^6 , 17.3 x 10^6, or 69.1 x 10^6, for 100 μm, 50 μm and 25 μm pitches respectively. In order to meet or exceed the resolving capabilities of screen-film mammography a 25μm detector element (del) pitch would be required, given that screen-film systems can resolve high contrast objects containing spatial frequencies approaching 20 mm^{-1}. Current digital mammography systems have detector apertures of nominal dimensions ranging between 40 μm and 100 μm . It is important to note however, that existing systems with the smaller pitches generally do not have a presampling MTF which warrants the small sampling pitch. Although at present there is no consensus on what del size is required there is some anecdotal evidence that characterization of microcalcifications is facilitated when the spatial resolution is increased. In any case, in the interpretation of mammograms, it is often desirable to produce images of certain suspicious areas of the breast with very high spatial resolution and we have, therefore, attempted to produce a detector with this capability. For situations when lower resolution is acceptable, this can easily be achieved by averaging the signals from adjacent dels.

For a variety of reasons, it is very difficult to create a full-field digital mammography system employing flat panel TFT arrays with a 25 μm del. Maintaining a high fill factor is one reason, and another is poor manufacturing yield, due to the obviously large number of dels. On the other hand, such a small del size on a slot-scanned system is technically tractable, in part, because the detector is smaller, so there will be fewer dels. While the slot-scan approach requires a specialized mechanical scanning apparatus and a longer image acquisition time, compared to flat-panel detector systems, and X-ray tube heat loading is much greater, it does have the benefit of dose-efficient scatter rejection and possibly lower detector cost. Typically, the detector used in such a system consists of a CsI(Tl) phosphor, fibreoptically coupled to multiple rectangular CCD arrays operated in time delay integration (TDI) mode. While this detector can produce excellent images, it suffers from some of the limitations common to all phosphor-based or indirect X-ray detectors. The main limitation is the need to compromise between detector thickness (and, therefore, its quantum interaction efficiency) and spatial resolution. This compromise occurs because the spread of light from the phosphor and the accompanying loss of resolution becomes more significant as detector thickness increases.

It is possible to overcome this problem by using a direct conversion detector in which the energy of absorbed x rays is immediately converted to electric charge carriers. In such detectors, an electric field normal to the image plane guides the signal charges directly to a collection electrode. There is little lateral displacement of the charges and the main factor affecting MTF should only be the aperture response function of the detector element (del). A number of direct conversion detector materials are currently under development, including silicon, a-Se, cadmium zinc telluride, mercury iodide, lead iodide, and gallium arsenide. Excellent results have been achieved using CZT indium bump bonded to CCD detectors.

However we are primarily interested in a-Se and CCDs as a readout method for slot scanned systems for these reasons:

1. The higher $W_{\pm}$ value of a-Se results in fewer charges and will not saturate the CCD detector, as would other X-ray photoconductors.
2. CCD readout noise is considerably lower than TFT arrays and should permit X-ray quantum noise limited readout even though the signal produced by the a-Se layer is reduced as compared to other photoconductors.
3. Whereas the a-Se is directly evaporated on the CCD charge collection electrode, and the charge collection electrode covers nearly all of the del area, a fill factor approaching 100% should be possible even for 25 μm x 25 μm dels.
4. The direct evaporation of a-Se onto the CCD readout structure is simple and cost effective compared to other techniques such as Indium bump bonding.

Here, we discuss the first steps towards the development of a slot-scanned detector based on an a-Se X-ray absorber, directly deposited on a simple linear CCD readout device.

Our work is proceeding along two parallel, but integrated paths: 1) the development and evaluation of CCD readout devices compatible with the direct evaporation of a-Se materials which transfer electron X-ray signal charges, and 2) the design, development and testing of TDI buttable CCD devices which have a-Se deposited upon them as single integrated device.

2. FEASIBILITY OF COUPLING A-SE TO A CCD READOUT DEVICE

2.1. Discussion

Previous direct conversion detectors for use in slot-scanning digital mammography bonded two separate devices: a readout CCD and a detector array. Both devices were comprised of discrete elements which had to be precisely aligned and mated. We wished to test the hypothesis that a-Se could be directly deposited onto a CCD readout device and that an *electron* (rather than hole) charge signal from the a-Se would be successfully transferred to the CCD readout elements. For this purpose the linear CCD designed was designed conservatively: although the sampling pitch in the linear transfer direction is 25 μm, the signal electrode is 1 mm long in order to develop

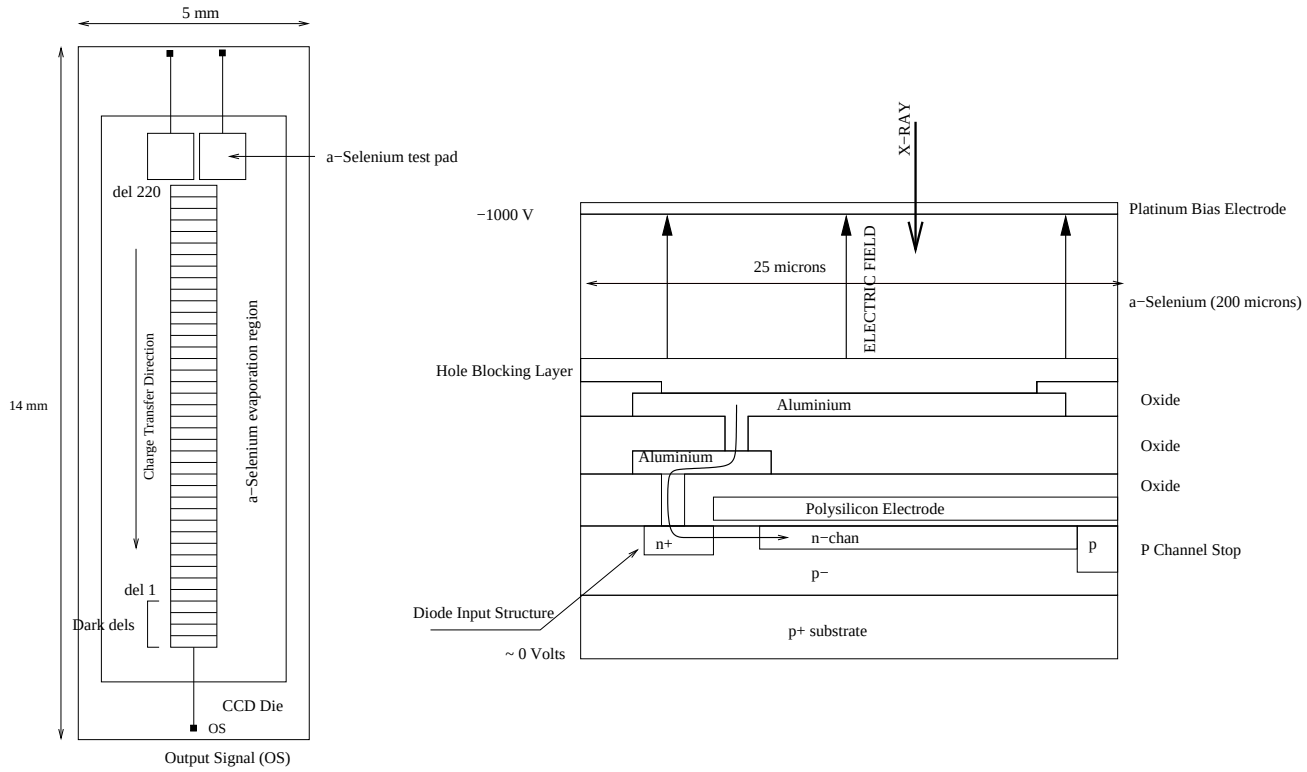

Figure 1. Simplified view (left) of the linear CCD die and a cross sectional view of part of a del (right). The CCD is a four phase buried channel device. The a-Se electron charge signal for each del enters the buried channel well via a diode structure located with the phase one clock stucture. The flow of electrons is represented with the curved line and arrow. Only the output signal (OS) bond pad is illustrated (black square) as well as two special bond pads (unrelated to CCD operation) useful for passively monitoring the bulk properties of the a-Se layer. The diagram is not to scale.

a large signal and each CCD storage element is 25 μm x 100 μm to accomodate the larger signal. For various reasons, including the higher hole mobility of holes than electrons in a-Se, image signals in a-Se detectors are often based on the collection of holes. However standard CCD design rules call for the collection of electrons. This requires the use of a negative bias on the surface of the a-Se where the x-rays are incident and the application of a suitable hole blocking layer at the CCD signal electrode-selenium interface. Without suitable blocking layers, unwanted large dark signals are injected into the a-Se bulk with the application of the large bias required to make the a-Se sensitive to x-rays. Please see a cross sectional view of a a-Se del and an illustration of the die structure in Fig. 1.

The input structure responsible for the transfer of x-ray signal charge to the CCD charge well is a small diode structure. A block diagram of the CCD functional structures is shown in Fig. 2 . The clocking structure is four phase and employs a single on-chip depletion-mode FET output which has a nominal bandwidth of 20 MHz. In practice the device was operated at 187 kHz and 3 MHz.

2.2. Required CCD Signal Capacity

The direct detection slot-scanned digital mammography detectors described by Mainprize et. al.[3,5] utilized photoconductors with $W_{\pm}$values of approximately 5 eV or less. Furthermore the $W_{\pm}$of those photoconductors (Si, CdZnTe,) are constant and independent of the applied electric field. In consideration of the relatively large exposures which may be necessary in mammography and the charge storage capability of nominal CCD design rules, Mainprize et. al. considered it necessary to design a CCD structure with 24 parallel sections to accomodate the large charge signal. We note that the $W_{\pm}$ of a-Se at mammographic energy ranges is 64 eV[6] at a field strength of 10 V/μm and varies with the field strength F [V/μm] according to the empirical expression[7]

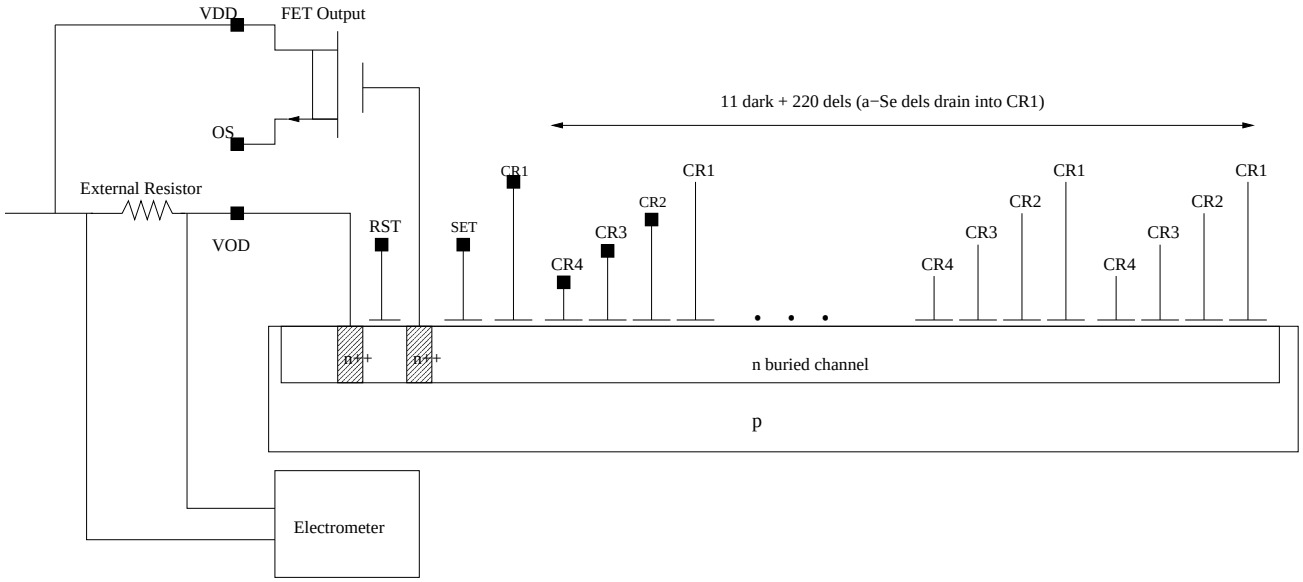

Figure 2. Simplified block diagram of the linear CCD. There are 220 dels with aluminium signal electrodes which interface to the a-Se layer. There are 11 dark dels which do not have aluminium signal electrodes. The dark dels are adjacent to the final output stage (left hand side of diagram) of the CCD. The signal charge is converted to a voltage by a floating diffusion output with reset. The device was designed with a special pin VOD, which allowed for the measurement of charge (via an external resistor) required to reset the floating diffusion output. This allowed for the direct measurement of the del well capacity by measuring the voltage drop across the external resistor shown in the left of the diagram.

$$W_{\pm} = W'(\frac{F}{10})^{-b} \tag{1}$$

where F is the electric field in V/μm, W' is the value of $W_{\pm}$at 10 V/μm, and b is a constant with a typical value of 2/3 . Whereas the $W_{\pm}$ of a-Se is more than 10x the value of Si, CdZnTe and other x-ray photoconductors, it should be possible to construct a slot-scanned detector for digital mammography using one or at most a few parallel sections. Furthermore, whereas the gain of a-Se can be controlled by varying F it may be possible to optimize the detector dynamically by altering F.

3. EXPERIMENTAL METHODS

The custom linear CCD was fabricated using a 2.5 μm process. Both a buried and a surface channel version of the linear CCD were fabricated, with a hope that the charge transfer efficiency (CTE) of the surface device would be adequate. Surface channel CCDs typically have a charge storage capacity three times that of buried channel devices, but typically suffer from poor CTE. The CCD devices were evaluated using a custom clocking circuit and a correlated double sampling (CDS) 14 bit data acquistion system. The CCD devices were thermally regulated at a temperature of 20 degrees Celsius.

The devices were exposed to an x-ray spectrum generated by a Tungsten target operated at a constant potential of 35 kV. The spectrum was filtered by 0.5 mm of Al and a Mo filter 0.02 mm thick. Using the methods of Tucker[8] et. al. the spectrum and its characteristics were estimated. The mean energy was estimated at 22.5 keV and the photon flux 5.1 x $10^4 \mathrm{mR}^{-1}\mathrm{mm}^{-2}$.

4. FULL WELL CHARGE CAPACITY

The full well charge capacity was calculated during the design of the CCD (6 x 10^6) and it was later measured estimated using two different techniques. In the first technique a device was exposed to a constant, weak source of visible light. The device did not have a-Se deposited upon it and was therefore sensitive to light. In the

Table 1. The estimation and experimental measurement of $Q_{del-sat}$, the full well number of charges held by a del.

CCD Design Estimation	Current Measurement Method	X-ray Signal Measurement and Method
6 x 10^6	5.9 x 10^6	5.1 x 10^6

free-run clock mode of operation (the mode which continuously refreshes and empties the dels) the device was clocked at frequency $\nu = 187$ kHz, giving a line readout time τ_l= 1.24 ms, based upon a line width of 231 (11 dark + 220 image) dels. The time τ_l is the time (in free-run clock mode) that any single del has to accumulate a signal charge. Under these conditions the voltage drop $\Phi_R$across resister R (1 M Ω) supplying current to the VOD pin (see Fig. 2), was measured using a Keithly model 35617 EBS programmable dosimeter. In the continuous readout mode the current is given by

$$i = \nu Q_{del} \tag{2}$$

where $Q_{del}$is the charge stored on each del.

It is possible, using the digital data acquisition system, to suspend the clocking of the CCD and make an exposure of any desired time duration. It was observed that an exposure of approximiately $\tau_{sat} = 56.6$ ms, caused the detector to saturate. Using Ohm's law, the saturation value of $Q_{del-sat}$can be estimated by

$$Q_{del-sat} = \frac{\Phi_R \tau_{sat}}{R \nu \tau_l} \tag{3}$$

which, using the observed value of $\Phi_R = 3.9$ mV, evaluates to 5.9 x 10^6q.

The second experimental method employed to determine $Q_{del-sat}$ was more indirect. An a-Se coated detector (a-Se thickness = 200 μm) was irradiated with x-rays, under bias such that $F = 2.5$ V/μm, and the exposure (mR) required to cause incipient saturation was 38.8 mR. Using the x-ray spectrum simulation methods referenced above, the energy deposited in the a-Se layer for the area (0.025 mm^{-2}) of a del was calculated. Using Eq. 1 the working value of $W_{\pm}$was evaluated and $Q_{del-sat}$ determined. The full well calculations and measurements are summarised in Table1 . It should be noted that $Q_{del-sat}$ is dependent upon the clock potentials, which for these measurements were 10 V.

5. CHARGE TRANSFER (IN)EFFICIENCY

The charge transfer efficiency CTE, is related to the charge transfer inefficiency ϵ, by $CTE = 1-\epsilon$. Following Janesick[9] the CTE was evaluated using the extended pixel edge response (EPER). As illustrated in Fig. 2 the linear CCD is comprised of 11 dark dels (not connected by a signal electrode to the a-Se layer) and 220 dels with electrodes connected to the a-Se layer. Extended pixels or dels refers to the "overclocking" of the detector which means that during a line readout, an excess of clock cycles is performed over the number required. The signal recovered in the extended dels is a residual signal due to incomplete charge transfer. For our purposes the CTE expression of Janesick has been approximated by

$$CTE = 1 - \frac{del_{n+1}}{< del_{sig} > n} \tag{4}$$

where $del_{n+1}$is the signal of the first overclocked del, $< del_{sig} >$ is the average signal of the non-overclocked dels (excluding the dark dels) and n is the number of transfers (231). Shown in Fig. 3 is the average response (several readouts) of a detector to a sequence of non-satururating x-ray exposures. Using Eq. 4 and the data from the plot of Fig. 3 a typical value of 0.9998 is evaluated. A small offset, plainly evident in the signal of the most overclocked dels, was subtracted from the signal values used in obtaining the values in Eq. 4 .

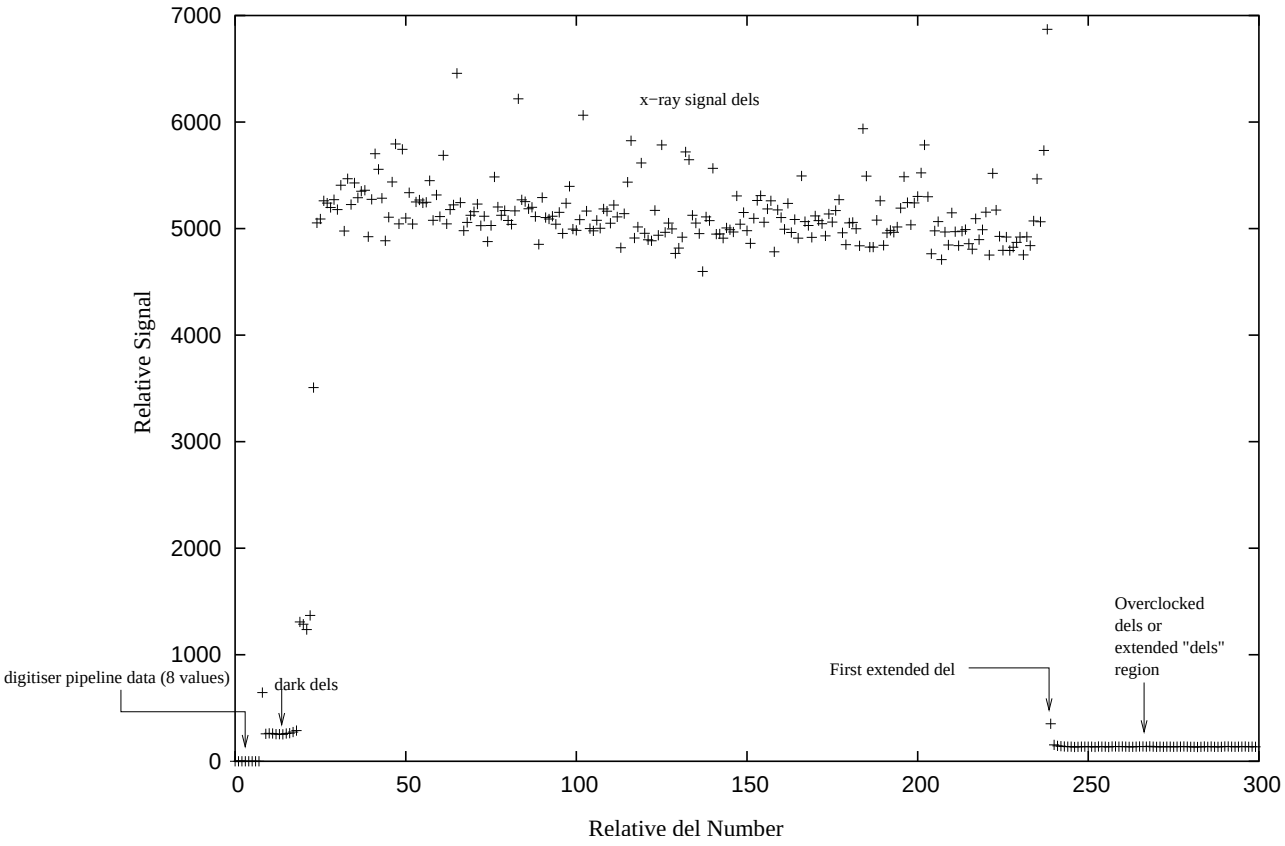

Figure 3. A plot of a detector readout line used in calculating the CTE. The plot is an average of several x-ray exposures. The large variation in response is due to the fixed pattern response (fpr) caused by intrinsic sensitivity variations of each del.

6. DARK SIGNAL

There are two sources of dark signal in the detector, that pertaining to the a-Se x-ray detection layer, and that pertaining to the operation of the CCD. The first source is associated with the a-Se detection regions and the second is comprised of, according to Janesick: (1) depeletion dark current, (2) surface dark current, and (3) substrate dark current. According to Janesick, the surface and depletion currents are the largest with values typically ranging from 60 pA/cm^{2}to 10 nA/cm^{2}and 3 pA/cm^{2}to 100 pA/cm^{2}respectively. Assuming a full well of 6 x 10^6q (Table1), CCD area = 2.5 x 10^{-3}mm^{-2}, and fill time of 13 s, one calculates a linear CCD dark current of 3.0 nA. This value is on the high side, and we expect that the CCD devices planned for TDI imaging will have a lower dark current.

In consideration of dark current generation, the a-Se based detector element (del) is comprised of six regions:

1. The X-ray side Platinum conductive electrode (negative bias)
2. An electron blocking layer adjacent to the Platinum electrode and a-Se
3. The primary a-Se x-ray detection layer
4. A a-Se hole blocking layer
5. An Aluminum electrode (positive bias) connected to the input structure of the CCD well
6. The CCD electron charge well

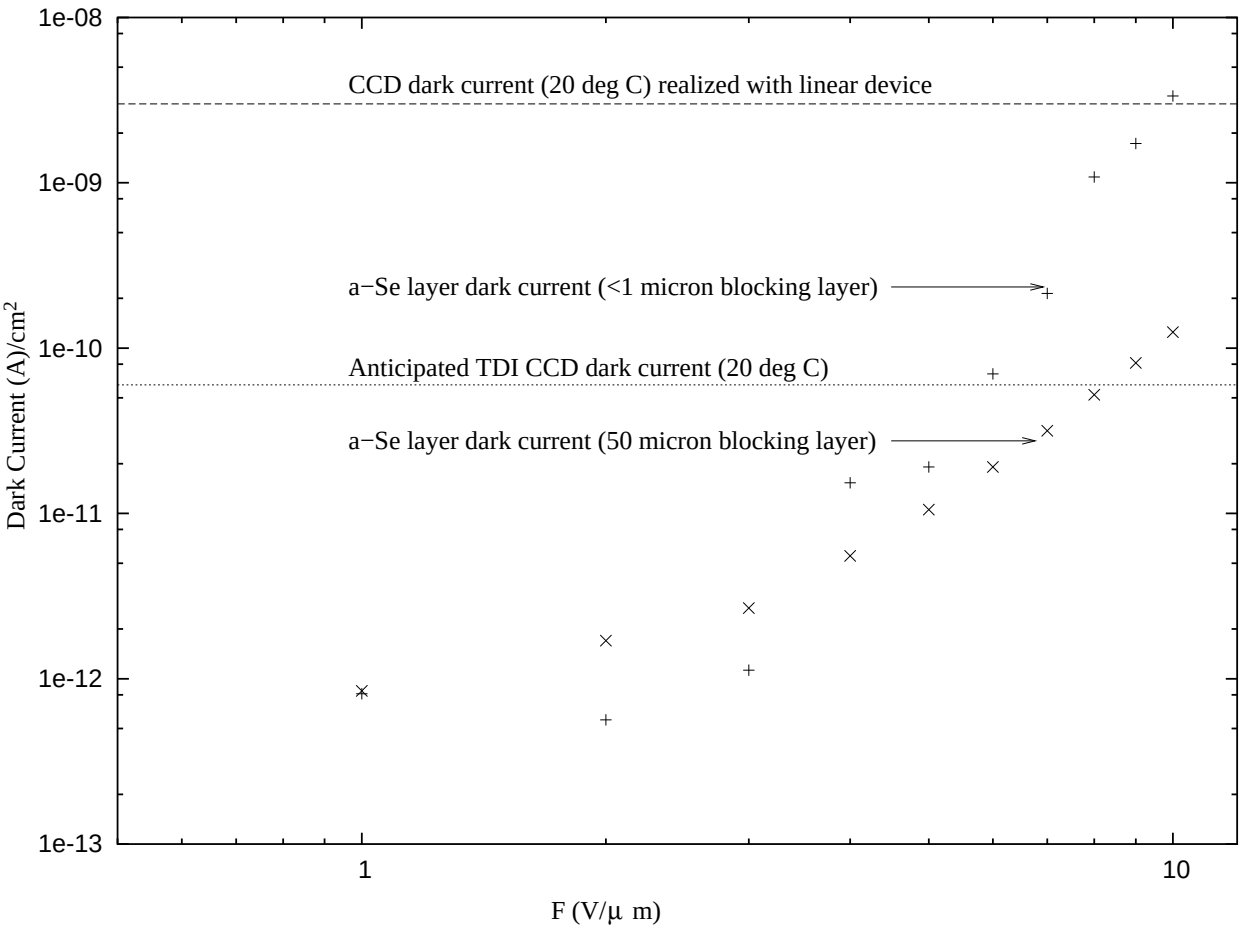

Figure 4. Dark current measurements on non-CCD "sister" samples. The sister samples had Aluminium substrates comparable to the CCD die. The dark current for the sample with the 50 micron blocking layer is somewhat better than for the sample with the much thinner ($\leq$ 1 micron) blocking layer. For reference is shown a typical intrinsic dark current due of the operation of the linear CCD. This dark current is not related to the a-Se layer. Additionally, the intrinsic dark current of the planned, area TDI, CCD detectors is anticipated to be smaller than for the linear device.

as illustrated in Fig. 6 . Due to temporary shortcomings of the arrangement used to bring the high voltage bias to the detector, the maximum bias potential applied was 500 V. However a-Se leakage currents were tested at much higher bias levels on "sister" samples, devices with comparable aluminium substrates as the CCD die. The results of measurements made on two samples with a thin ($\leq$1 μm blocking layer) and one with a thicker (50 μm) blocking layer are shown in Fig. 4 .

The previous direct detector slot-scan CCDs described by Mainprize depended upon a custom CCD fabrication process utilizing an n-type substrate resulting in a configuration with holes as the charge carriers. This arrangement is convenient, because for a-Se, hole transport is better than electron transport, and additionally the biasing arrangement (top x-ray side of a-Se positively biased) typically leads to lower a-Se leakage currents. However standard CCD processes utilize a p-type substrates, resulting in electrons as the charge carriers. In order to avoid costly and lengthy design cycles based upon non-standard processes, standard processes have been adopted, which in turn has necessitated the inversion of the biasing arrangement, and the development of novel a-Se blocking layers, in particular at the interface between the aluminium CCD signal collection electrode and the a-Se layer (region 5 of the above list).

The bulk region of the a-Se (region 3) will contribute very little to the dark current due to the intrinsic high

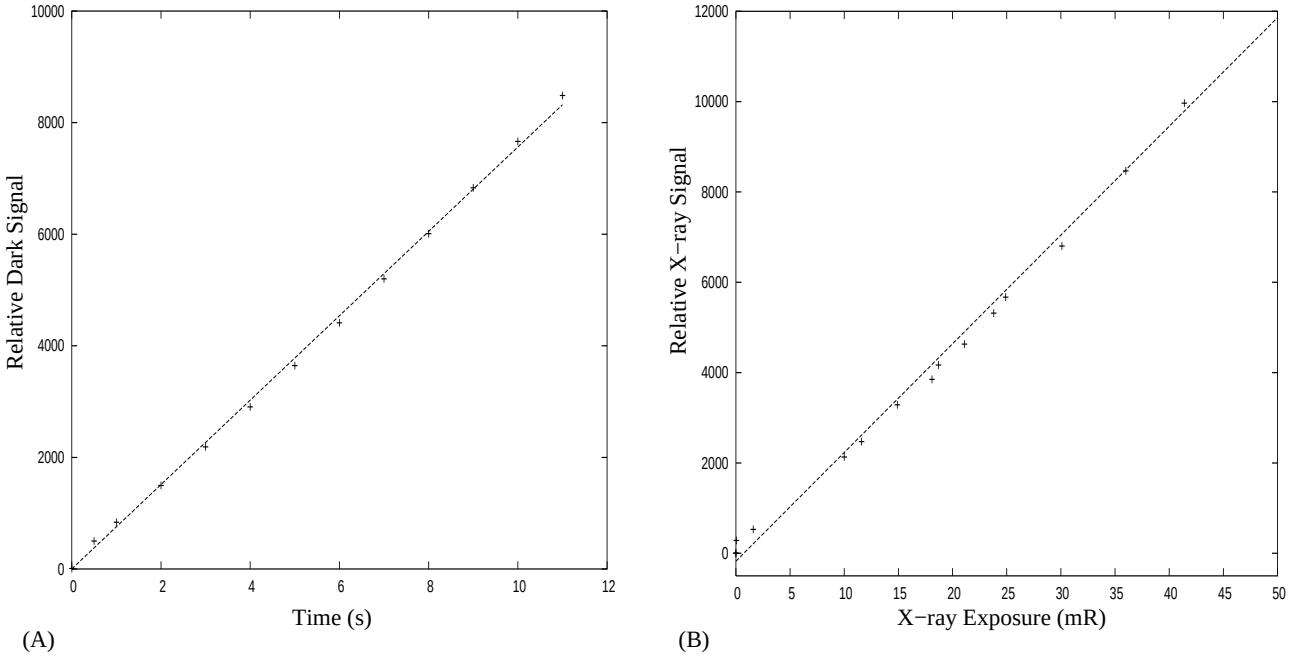

Figure 5. Plots of dark signal (integrated dark current) (A) and x-ray signal (B). The points are data, the lines are a linear fit to the data. The dark signal was obtained at 20 degrees Celsius and with no bias applied to the a-Se layer. Incipient saturation, as caused by the dark current, was noted at an integration time of 13 s. The x-ray signal was obtained with the a-Se layer biased such that $F = 2.0$ V/μm. The a-Se layer was 200 μm thick. The estimated mean energy of the incident x-ray spectrum was 23.9 keV. The x-ray exposures were sufficiently short that the contribution of dark signal was not significant.

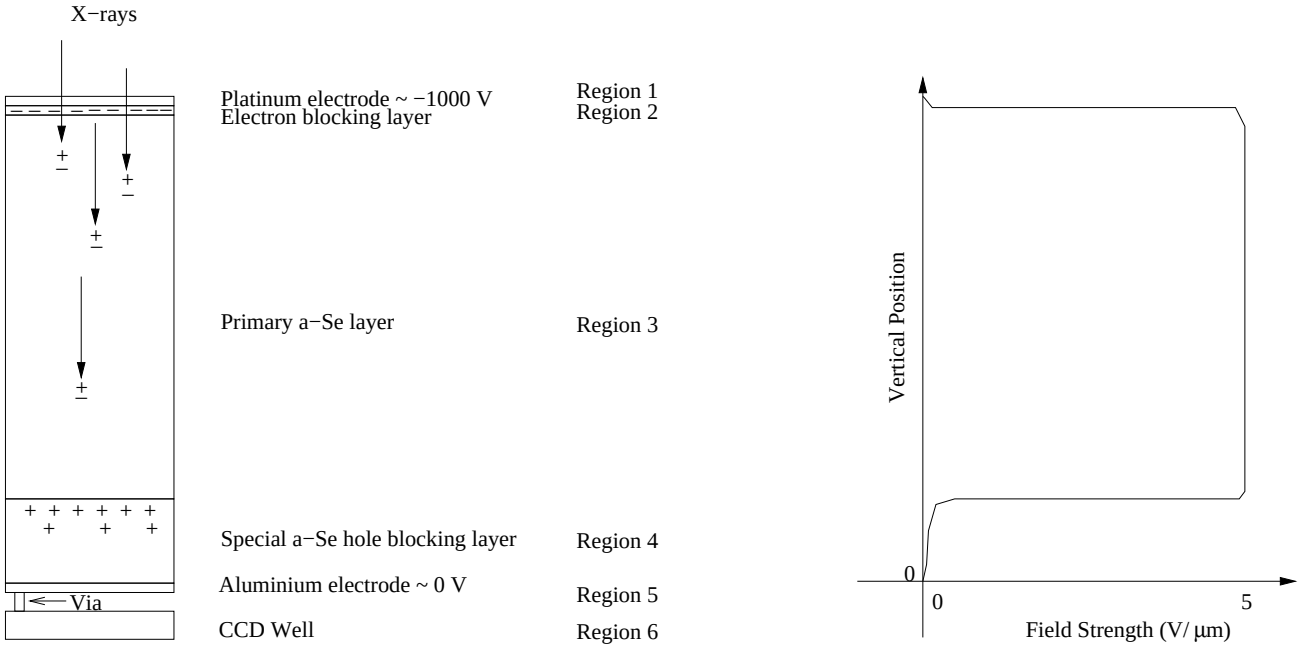

Figure 6. Regions of dark signal origin (left) and the corresponding electric field profile (right).

resistivity (very few thermally generated free carriers) of a-Se. However it is necessary to bias the a-Se, to make it x-ray sensitive, and of course extract the x-ray signal charge generated in region 3. This is done with metal contacts. There is no choice with the metal for the bottom positive CCD bias electrode, it must be aluminium, as dictated by CCD fabrication. Under the bias conditions shown in Fig. 6 , the CCD collection electrode will accept electrons, or viewed another way, inject holes. Because the transport of holes in a-Se is naturally rather good, this can result in a large dark signal. Conceptually, one might suppose that one way of suppressing the charge injection rate would be to reduce the electric field at the interface between the metal electrode and the a-Se. With this in mind we created blocking layers on the CCD Aluminium signal electrodes with a high number of hole traps. We then suppose that the accumulation of trapped holes lowers the vertical electric field in a manner shown in Fig. 6 . Furthermore, we suggest that the greatest density of trapped charge occurs near the boundary of the hole trapping layer, region 4, and the bottom of region 3, the x-ray sensitive region.

7. X-RAY SIGNAL RESPONSE

It is anticipated that an a-Se layer 200 μm thick will be sufficient to absorb at least 90 % of the incident x-ray energy with the type of mammographic x-ray spectrum encountered in slot-scanned systems. Shown in Fig. 5 (B) is the measured x-ray response.

8. THE MTF AND ITS DEPENDENCE ON BLOCKING LAYER THICKNESS

8.1. Theory

As discussed in the section on dark signal, we have employed hole blocking layers to reduce dark currents. Initially on the first samples, the blocking layers were made rather thick, i.e. 50 μm. But it was soon realized that the MTF was lower than expected based upon the theoretical predictions of Que and Rowlands[10] . It was suspected that the MTF was being reduced by electrostatic blurring effects related to the hole trapping layer. The basic physical concept of MTF reduction is depicted in Fig. 7 , which is essentially the model proposed by Zhao[11]et al. who proposed that the electrostatic blurring would be given by

$$T_b(\nu) = \frac{Lsinh[2\pi\nu(L-l)]}{(L-l)sin(2\pi\nu L)} \tag{5}$$

where L is the combined thickness of the primary a-Se and blocking layers and the assumption is made that the image charge resides at the top (x-ray side) of the blocking layer. The MTF will also be reduced by the CTE as approximated by:

$$C_b(\nu) = e^{-n\epsilon[1-cos(2\pi\nu p)]} \tag{6}$$

where $\nu$is the spatial frequency, p is the sampling pitch (25 μm), and n is the number of transfers (231). Eq. 6 is an approximation given by Theuwissen[12] when $\epsilon \ll 1$. The MTF as measured by our discrete detector with sampling pitch p will also be modified by the sinc function

$$S(\nu) = \frac{sin(\pi\nu p)}{(\pi\nu p)} \tag{7}$$

.

Que and Rowlands[10] showed that at mammographic energies the MTF in a-Se would be reduced by k fluorescence escape. Following their methods, detailed calculations were carried out to estimate the true unsampled MTF which we shall denote by MTF(ν). Finally we can express the expected value of the measured MTF$_m(\nu)$ by:

$$MTF_m(\nu) = MTF(\nu)T_b(\nu)C_b(\nu)S(\nu) \tag{8}$$

.

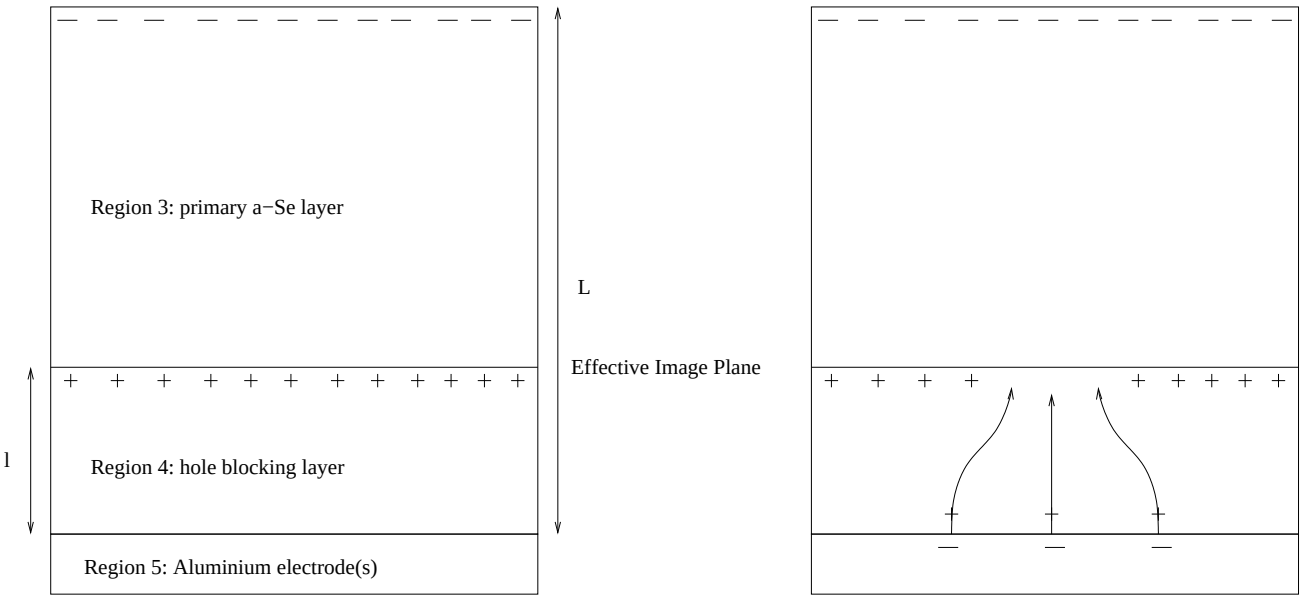

Figure 7. Effective image plane created by the hole blocking layer, wherein it is assumed most of the trapped holes reside at the interface between the blocking layer and the primary a-Se detection layer. When negative image charge is created in the primary layer, it initially moves to and nulls positive charge at the top blocking layer interface, creating an effective region of negative charge. A positive mirror charge is induced on the del Aluminium electrodes which results in electric field bending due to the separation l between the del electrodes and the top blocking layer interface.

8.2. Experiment

Because the linear detector has only one row of detectors, it was not possible to apply the slanted edge technique. The MTF was measured using an edge, and in order to super sample the edge to avoid aliasing effects, a supersampled response was synthesized from 22 multiple edge scans, each separated by p/22. The focal spot size of the x-ray tube was specified as having a nominal dimension of 0.1 mm, the distance from the focal spot to the image plane was 65 cm, and the separation between the edge and image plane was 2 mm. The effects of focal spot blurring are expected to be insignificant.

The supersampled edge for the sample with ~ 0 μm blocking layer is shown in Fig. 8 . The MTF from the supersampled edge was determined by differentiating the edge data and then taking the magnitude of Fourier transform, properly normalized. Because the data was noisy, the non-linear optimization method of Maidment and Albert[13] was used to great advantage before taking the derivative. The MTF data for devices with blocking layers of thickness ~ 0, 16, 30 and 51 μm are shown in Fig. 9 . The experimentally derived MTF is mainly in agreement with the theoretical predictions except for the device with the 16 μm blocking layer. The discrepancy is consistent with an improper formed blocking layer in which the trapped charge density is low or more evenly distributed than suggested by Fig. 6 .

9. SUMMARY AND CONCLUSIONS

We have shown that it is possible to make a high resolution x-ray detector by directly depositing a-Se onto a specially designed linear CCD. We have demonstrated that the device has a full well capacity of approximately 6 x 10^6q and that the x-ray response is consistent with the value of $W_{\pm}$as given by Stone[6] et al. at mammographic energies. We have demonstrated that the CTE is sufficiently high to prevent significant loss of resolution at 20 $mm^{-1}$for a device have 231 transfer steps. We have demonstrated that it is possible to make specialized blocking layers which suppress the a-Se dark currents at high bias fields (10 V μm^{-1}) to levels lower than intrinsic dark current of the CCD, and hence small enough for slot-scanned operation where the typical effective dark current integration time is of the order of 300 ms. We have demonstrated that the blocking layers reduce the resolution of the device in a manner which is approximately consistent with the theory outlined.

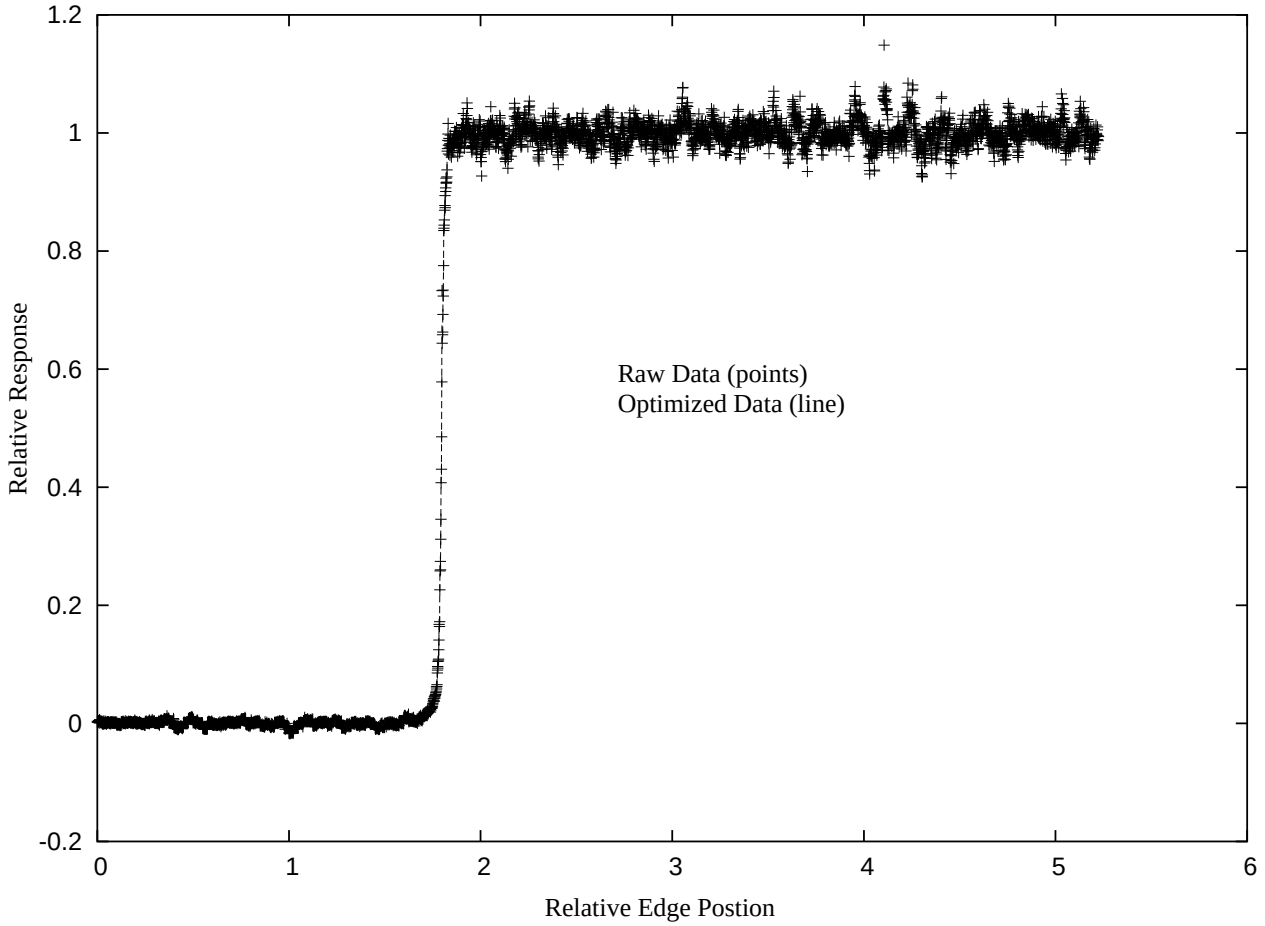

Figure 8. Supersampled edge for 0 μm blocking layer thickness sample.

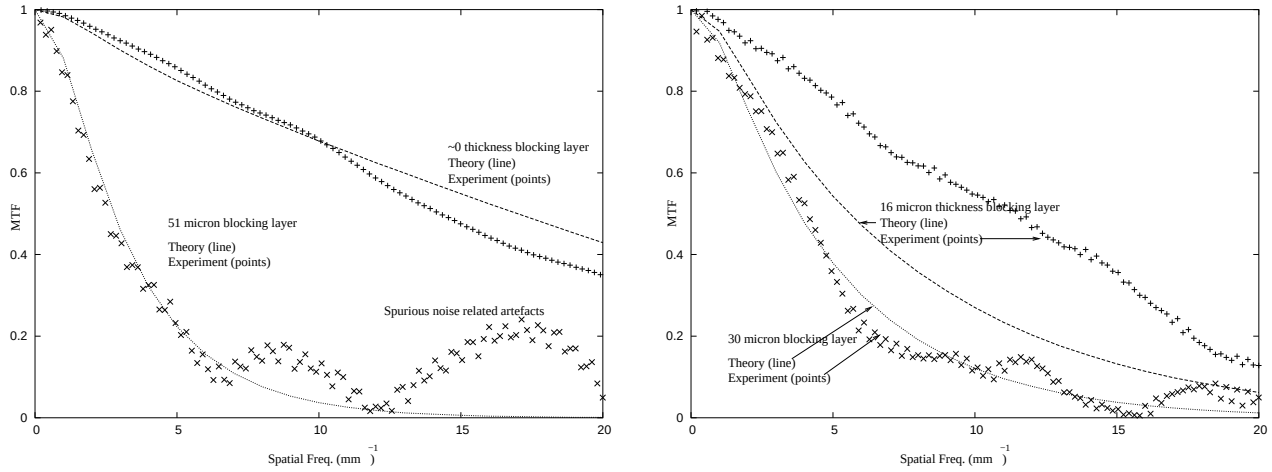

Figure 9. Calculated and measured MTF for blocking layers of 0,16,30 and 51 μm.

REFERENCES

1. A. D. A. Maidment, *Scanned-Slot Digital Mammography.* PhD thesis, University of Toronto, 1993.
2. A. D. A. Maidment, B. G. Starkoski, I. C. Soutar, G. E. Mawdsley, D. B. Plewes, and M. J. Yaffe, "A clinical scanned-slot digital mammography prototype," *Radiology* **185**, p. 249, 1992.
3. J. G. . Mainprize, N. L. Ford, S. Yin, T. Tumer, and M. J. Yaffe, "A slot-scanned photodiode-array/ccd hybrid detector for digital mammography," *Med. Phys.* **29**, pp. 214–255, 2002.
4. J. Beutel, H. L. Kundel, and R. L. VanMetter, *Handbook of Medical Imaging Volume I. Physics and Psychophysics*, SPIE Press, Bellingham, Washington 98227-0010, 2000.
5. J. G. Mainprize, N. L. Ford, S. Yin, E. E. Gordon, W. J. Hamilton, T. Tumer, and M. J. Yaffe, "A cdznte slot-scanned detector for digital mammography," *Med. Phys.* **29**, pp. 2767–2781, 2002.
6. M. F. Stone, W. Zhao, B. V. Jacak, P. O'Connor, B. Yu, and P. Rehak, "The x-ray sensitivity of amorphous selenium for mammography," *Med. Phys.* **29**, pp. 319–324, 2002.
7. D. Mah, J. A. Rowlands, and J. A. Rawlinson, "Sensitivity of amorphous selenium to x rays from 40 kvp to 18 mv: Measurements and implications for portal imaging," *Med. Phys.* **25**, pp. 444–456, 1998.
8. D. M. Tucker, G. T. Barnes, and D. P. Charkraboty, "Semiempirical model for generating tungsten target x-ray spectra," *Med. Phys.* **18**, pp. 211–218, 1991.
9. J. R. Janesick, *Scientific Charge-Coupled Devices*, SPIE Press, 2001.
10. W. Que and J. A. Rowlands, "X-ray imaging using amorphous selenium: Inherent spatial resolution," *Med. Phys.* **22**, pp. 365–374, 1995.
11. W. Zhao, W. G. Ji, A. Debrie, and J. A. Rowlands, "Imaging performance of amorphous selenium based flat-panel detectors for digital mammography: Characterization of a small prototype detector," *Med. Phys.* **30**, pp. 254–263, 2003.
12. A. J. P. Theuwissen, *Solid-State Iimaging with Charge-Coupled Devices*, Kluwer Academic Publishers, 1995.
13. A. D. A. Maidment and M. Albert, "Conditioning data for calculation of the modulation transfer function," *Med. Phys.* **30**, pp. 248–253, 2003.